

# CHALMERS



## The effects of the power amplifier on wideband radar signals

*Master of Science Thesis*

SEBASTIAN HOLMQVIST  
JOHN DAHL

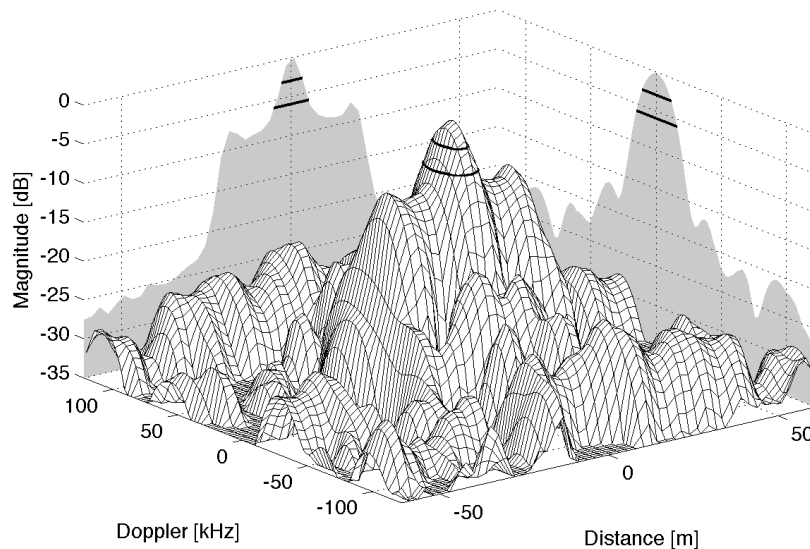
Department of Signals and Systems  
*Division of Signal Processing*  
CHALMERS UNIVERSITY OF TECHNOLOGY  
Göteborg, Sweden, 2013  
Report No. EX020/2013



Issued by  
John Dahl and Sebastian Holmqvist  
Classification - Export Control  
NOT EXPORT CONTROLLED

Date 2013-06-11 Issue A Document ID EX020/2013  
Classification - Company Confidentiality  
UNCLASSIFIED  
Classification - Defence Secrecy  
ÖPPEN/UNCLASSIFIED

## THE EFFECTS OF THE POWER AMPLIFIER ON WIDEBAND RADAR SIGNALS



This document and the information contained herein is the property of Saab AB and must not be used, disclosed or altered without Saab AB prior written consent.

Supervisors: Kent Falk and Marie Ström  
Examiner: Tomas McKelvey  
CHALMERS UNIVERSITY OF TECHNOLOGY  
Gothenburg, Sweden 2013



Issued by  
John Dahl and Sebastian Holmqvist  
Classification - Export Control  
NOT EXPORT CONTROLLED

Date                      Issue                      Document ID  
2013-06-11            A                              EX020/2013  
Classification - Company Confidentiality  
UNCLASSIFIED  
Classification - Defence Secrecy  
ÖPPEN/UNCLASSIFIED

---

### Abstract

Recent work in scenario-optimal wideband *Multiple Input Multiple Output* (MIMO) radar signals have spurred the idea of wideband, adaptive radar systems. For the sake of detection range, these scenario-optimal signals can be optimized against a low *Peak to Average Power Ratio* (PAPR). However, theoretical gains in *Signal to Interference and Noise Ratio* (SINR) could prove pointless if the signals are distorted by the *Power Amplifier* (PA). This thesis serves to answer the question: does the overall linearity of the PA degrade for scenario-optimal wideband MIMO radar signals – in particular those optimized against a low PAPR?

A comprehensive measuring rig was constructed and was highly automated to ensure repeatability. By analyzing the signals before and after the class A-B PA of interest, the classic target detection (doppler and distance) is first evaluated using the *Wideband Ambiguity Function* (WAF). The processed scenario-optimal wideband MIMO radar signals are then evaluated against a scenario-matched filter and compared to a pre-calculated SINR.

The results show that classic target detection is largely insensitive to the effects of the PA, even when running the PA at compression levels. Scenario-optimal wideband MIMO radar signals are however highly susceptible to distortion. Further work is promoted and pre-distortion is proposed as a possible solution.



# SAAB

MASTER THESIS

3 (40)

Issued by  
John Dahl and Sebastian Holmqvist  
Classification - Export Control  
NOT EXPORT CONTROLLED

Date                      Issue                      Document ID  
2013-06-11      A                      EX020/2013  
Classification - Company Confidentiality  
UNCLASSIFIED  
Classification - Defence Secrecy  
ÖPPEN/UNCLASSIFIED

---

## Preface

This master thesis was written during the spring of 2013 at the Department of *Signals and Systems* at *Chalmers University of Technology* (Chalmers), Gothenburg. The research and development was carried out at Saab EDS, Gothenburg and was supervised by Kent Falk and Marie Ström. The examiner at Chalmers was Tomas McKelvey.

The authors would like to thank Kent for all of his support and guidance. Also, Marie for her helpful thoughts and long Skype sessions. Finally, Tomas for his thorough eyes. We would also like to thank Per, Henrik, Hannes and others, for their aid and suggestions.



Issued by  
John Dahl and Sebastian Holmqvist  
Classification - Export Control  
**NOT EXPORT CONTROLLED**

Date                    Issue                    Document ID  
2013-06-11    A                    EX020/2013  
Classification - Company Confidentiality  
**UNCLASSIFIED**  
Classification - Defence Secrecy  
**ÖPPEN/UNCLASSIFIED**

## Contents

<b>1</b>	<b>Introduction</b>	<b>6</b>
<b>2</b>	<b>Technical Background</b>	<b>8</b>
2.1	Power Amplifier Classes . . . . .	8
2.2	Peak to Average Power Ratio . . . . .	8
2.3	Ambiguity Function . . . . .	10
2.4	I/Q Modulation . . . . .	11
<b>3</b>	<b>Methodology</b>	<b>14</b>
3.1	Measuring Rig . . . . .	14
3.1.1	Equipment . . . . .	14
3.1.2	File Structure . . . . .	15
3.2	Signal Processing . . . . .	15
3.3	Validation . . . . .	16
<b>4</b>	<b>Implementation</b>	<b>17</b>
4.1	Measurement Analysis . . . . .	17
4.2	Signal Analysis . . . . .	19
4.2.1	Pre-processing . . . . .	19
4.2.2	Signal Process . . . . .	20
4.2.3	Post-processing . . . . .	20
4.2.4	WAF Implementation . . . . .	20
<b>5</b>	<b>Results</b>	<b>22</b>
5.1	Narrowband Linearity . . . . .	22
5.2	Target Ambiguity . . . . .	25
5.3	WAF Validation . . . . .	29
5.4	MIMO Analysis . . . . .	33
<b>6</b>	<b>Analysis</b>	<b>35</b>
6.1	Narrowband . . . . .	35
6.2	Ambiguity . . . . .	36
6.3	MIMO . . . . .	37
<b>7</b>	<b>Conclusions</b>	<b>38</b>
<b>A</b>	<b>Equipment</b>	<b>40</b>

This document and the information contained herein is the property of Saab AB and must not be used, disclosed or altered without Saab AB prior written consent.



Issued by  
John Dahl and Sebastian Holmqvist  
Classification - Export Control  
NOT EXPORT CONTROLLED

Date                      Issue                      Document ID  
2013-06-11              A                              EX020/2013  
Classification - Company Confidentiality  
UNCLASSIFIED  
Classification - Defence Secrecy  
ÖPPEN/UNCLASSIFIED

---

## Nomenclature

ADC	Analog to Digital Converter
ENOB	Effective Number Of Bits
CDMA	Code Division Multiple Access
CFR	Crest Factor Reduction
DAC	Digital to Analog Converter
GPIB	General Purpose Interface Bus
HT	Hilbert Transform
I/Q	In-phase/Quadrature
LSB	Least Significant Bit
MIMO	Multiple Input Multiple Output
NAF	Narrowband Ambiguity Function
OFDM	Orthogonal Frequency-Division Multiplexing
PA	Power Amplifier
PAPR	Peak to Average Power Ratio
PWM	Pulse Width Modulation
RADAR	RAdio Detection And Ranging
SINR	Signal to Interference and Noise Ratio
SNR	Signal to Noise Ratio
WAF	Wideband Ambiguity Function
ZOH	Zero Order Hold



Issued by  
John Dahl and Sebastian Holmqvist  
Classification - Export Control  
NOT EXPORT CONTROLLED

Date 2013-06-11 Issue A Document ID EX020/2013  
Classification - Company Confidentiality  
UNCLASSIFIED  
Classification - Defence Secrecy  
ÖPPEN/UNCLASSIFIED

## 1 Introduction

Traditionally, *RA*dio *D*etection *A*nd *R*anging (radar) operates by transmitting and receiving burst series of narrowband signals. In later years, increasingly complex mission scenarios have spurred the idea of wideband, adaptive radar systems. Recent work in scenario-optimal *M*ultiple *I*nput *M*ultiple *O*utput (MIMO) wideband radar theory [6] aims to generate signals matched against these complex scenarios (see Figure 1). By evolving from “classic” narrowband signals to more wideband signals it is possible to classify and identify specific targets even more efficiently, counteract jamming/interference, etc. This novel concept poses new challenges on both new advanced algorithms and hardware design.

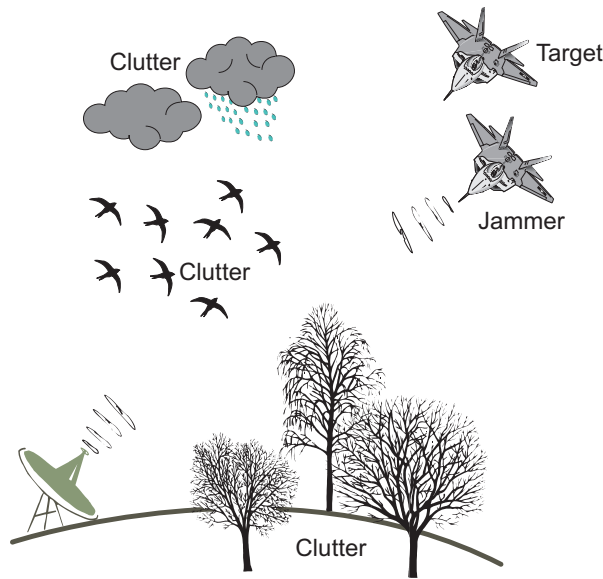


Figure 1: Overview of a complex radar scenario. [6]

Before implementing any of these optimal wideband signals, it is necessary to investigate the effects the *P*ower *A*mplifier (PA) has on the signal properties. This claim is also relevant for other “modern”, pre-existing, wideband signals such as CDMA, OFDM, etc. The gain in *S*ignal *t*o *I*nterference and *N*oise *R*atio (SINR) from using MIMO technology and scenario-optimal signals could all prove pointless if the transmitted signals are heavily distorted by the PA.

An important aspect is range. For radar receivers, the transmission level translates to range of detection. In telecommunications, engineers have long worked



Issued by  
John Dahl and Sebastian Holmqvist  
Classification - Export Control  
NOT EXPORT CONTROLLED

Date                      Issue                      Document ID  
2013-06-11              A                              EX020/2013  
Classification - Company Confidentiality  
UNCLASSIFIED  
Classification - Defence Secrecy  
ÖPPEN/UNCLASSIFIED

---

hard at so called *Crest Factor Reduction* (CFR). A smaller CFR generally allows for a higher bitrate in transceiver hardware. Its power factor equivalent, *Peak to Average Power Ratio* (PAPR), relates to power efficiency. A signal with a low PAPR allows for a minimal dynamic range in the amplifier, thus driving down hardware cost. Or similarly, maximizing output power as the average power is higher.

This thesis serves to answer the question: does the overall linearity of an class A-B PA degrade for scenario-optimal wideband MIMO radar signals – in particular those optimized against PAPR?

In order to answer the question stated above, scenario-optimized signals must be realized, processed and analyzed before and after passing the PA. As a way to emulate the inner workings of a non MIMO radar, the *Ambiguity function* is used to evaluate how the target ambiguity is affected by comparing the signal before and after passing the PA.

Another way to evaluate the loss of performance would be to investigate how the scenario-optimal MIMO signals affects the calculated SINR. Note that the optimal signals are produced by the method described in [7], where properties of the transmitted signals and receiver filters are derived to maximize the SINR for a pre-specified scenario. The processed signals would then be evaluated for the specified scenario using the already optimized receiver filter, based on a perfectly linear PA.



Issued by  
John Dahl and Sebastian Holmqvist  
Classification - Export Control  
NOT EXPORT CONTROLLED

Date                      Issue                      Document ID  
2013-06-11      A                      EX020/2013  
Classification - Company Confidentiality  
UNCLASSIFIED  
Classification - Defence Secrecy  
ÖPPEN/UNCLASSIFIED

---

## 2 Technical Background

This section introduces the reader to some of the basics in PA theory, the concept of PAPR, radar target detection, and *In-phase/Quadrature* (I/Q) signal modulation.

### 2.1 Power Amplifier Classes

PAs are grouped by a number of classes. The class specifications dictate power efficiency and inherently affect amplifier linearity. There are basically four main classes.

The A class is defined as “biased”. In other words, an voltage offset causes current to always flow in the circuit, which translates to the PA being “always on”. Due to this offset, there are no power-on transients. As a result, the amplifier operates inherently linear. On the downside, the power efficiency is typically well below 50 % [4].

A typical B class PA consists of a push-pull dual circuitry where one circuit amplifies the positive voltage of a signal and the other amplifies the negative voltage. The power efficiency can theoretically be as high as 78.5% [4]. Unfortunately, this technique can cause severe crossover distortions to the output signal when switching between the two circuits.

Typically referred to as “digital”, the D class differs by being a purely switched circuit. In terms of power efficiency, its *Pulse Width Modulation* (PWM) technique is the most efficient one, compared to the other PA classes. However, due to the PWM square wave operation, large harmonics can arise and subsequently cause distortions to the output signal.

The A-B class is basically a version of the B class but with a small bias added. The resulting current bias introduces a range overlap between the two circuits which basically mitigates the crossover nonlinearities. The A-B class also exists as a single circuit device, with the drawback of not being perfectly symmetric. Compared to the B class, the main trade off is with the power efficiency. [4]

### 2.2 Peak to Average Power Ratio

The term crest-factor originates from the early days of electrical engineering. The crest-factor was first coined by Dr. Gisbert Kapp [9] and is defined as the



Issued by  
 John Dahl and Sebastian Holmqvist  
 Classification - Export Control  
 NOT EXPORT CONTROLLED

Date 2013-06-11 Issue A Document ID EX020/2013  
 Classification - Company Confidentiality  
 UNCLASSIFIED  
 Classification - Defence Secrecy  
 ÖPPEN/UNCLASSIFIED

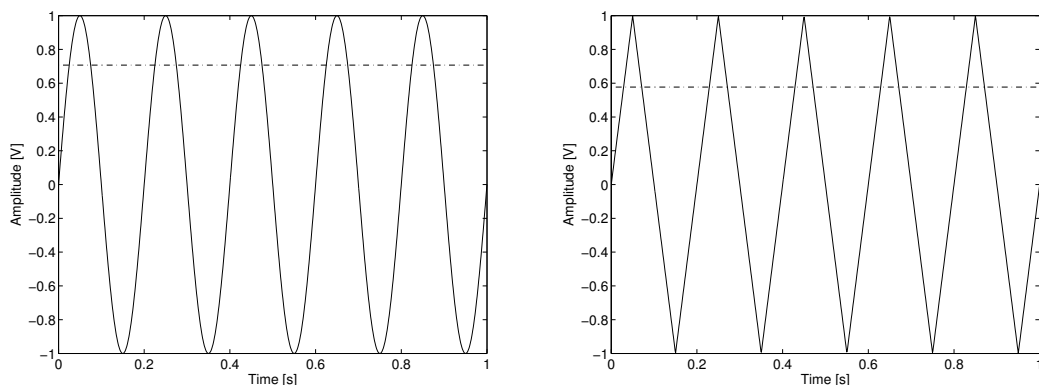
ratio between the peak signal amplitude and the average signal amplitude. A lower crest-factor yields a signal with a lower peak amplitude for a fix average amplitude. By squaring the crest-factor, it can be expressed as a ratio of power instead of amplitude and is then denoted as the *Peak to Average Power Ratio* (PAPR) and is formally expressed as

$$PAPR = \frac{|V|_{peak}^2}{V_{rms}^2}, \tag{1}$$

where  $V$  is the instantaneous amplitude of a signal.

Amplifiers can behave both as hard saturaters, denoted *clipping*, or soft saturaters, denoted *compression*. As the input power level increases, the gain increases linearly. For clipping,  $dV_{out}/dV_{in}$  is constant as  $V_{in} < V_{lim}$  and  $V_{out} = V_{lim}$  when  $V_{in} \geq V_{lim}$ . For compression,  $dV_{out}/dV_{in}$  slowly decreases towards zero as the PA goes into compression. When the gain has dropped 1 dB compared to it linearly increasing, it is said to have reached the 1 dB compression point.

The PAPR of a signal also serves as a good indicator of how constant its power envelope is. For example, a high power signal at 100 W, with a PAPR of 3 dB, means that the insulation and the components of a device have to withstand at least 200 W of peak power. A lower PAPR reduces saturation and some of the nonlinearities coupled with the saturation, given that the average power level stays the same. For a transmitter, a low PAPR translates to a higher power efficiency.



(a) A 5 Hz sinusoid wave.

(b) A 5 Hz sawtooth wave.

Figure 2: Two signals plotted with their respective RMS value.



Issued by  
John Dahl and Sebastian Holmqvist  
Classification - Export Control  
NOT EXPORT CONTROLLED

Date 2013-06-11 Issue A Document ID EX020/2013  
Classification - Company Confidentiality  
UNCLASSIFIED  
Classification - Defence Secrecy  
ÖPPEN/UNCLASSIFIED

A sinusoid and a sawtooth signal are plotted in Figure 2. Using the definition in (1), the signal RMS values of 0.707 and 0.577 translates to a PAPR of 3.01 dB and 4.77 dB respectively. For two signals with the same peak value, a larger PAPR, e.g., for the sawtooth wave, translates to a lower RMS value, i.e., a shorter range of detection.

### 2.3 Ambiguity Function

Classic radar rely on accurate readings of both *time delay* and *Doppler time scaling*. The reference signal,  $f(t)$ , is defined as

$$f(t) = s(t)e^{j\omega_c t}, \quad (2)$$

where  $s(t)$  denotes a baseband signal modulated onto a carrier wave at angular frequency  $\omega_c$ . For narrowband signals, assuming  $|v/c| \ll 1$ , where  $v$  is the target object velocity and  $c$  is the signal propagation speed, the time delay and the Doppler effect on the received signal response,  $g(t)$ , can be approximated as

$$g(t) \approx f(t - \tau_0)e^{j\omega_{d0}t}, \quad (3)$$

where  $\omega_{d0} \approx (k_0 - 1)\omega_c$  and the Doppler scaling factor is approximated as  $k_0 \approx 1 - \frac{2v}{c}$ . The parameter  $\tau_0$  denotes the time delay [10].

In order to determine the accuracy of the correlation between two signals, e.g, a transmitted and a received signal, a sensitivity analysis is called for. Introducing the concept of the *ambiguity function* [11] allows to investigate the parameter sensitivity of two signals in the dimensions of both time delay and Doppler. The *Narrowband Ambiguity Function* (NAF) [12] is defined as

$$NAF_{f,g}(\omega_d, \tau) = \int_{-\infty}^{\infty} f(t - \tau)e^{j\omega_d t} g^*(t) dt. \quad (4)$$

Here,  $g^*(t)$  is the complex conjugate of the received signal response. A global maxima occurs when  $\omega_d = \omega_{d0}$  and  $\tau = \tau_0$ . However, the narrowband signal theory only applies as long as the *narrowband condition* [10] is fulfilled, i.e.,

$$\frac{2v}{c} \ll \frac{1}{TB}. \quad (5)$$

Issued by  
 John Dahl and Sebastian Holmqvist  
 Classification - Export Control  
 NOT EXPORT CONTROLLED

Date 2013-06-11 Issue A Document ID EX020/2013  
 Classification - Company Confidentiality  
 UNCLASSIFIED  
 Classification - Defence Secrecy  
 ÖPPEN/UNCLASSIFIED

In (5),  $TB$  is the time-bandwidth product of the signal. For signals with large fractional bandwidth,  $B/f_c$ , i.e., wideband signals, or signals with large relative object-to-propagation velocity ( $v/c$ ), e.g., sound waves, the narrowband condition is consequently violated. As a result, the Doppler frequency shift is no longer a valid approximation of the Doppler time scaling effect. Redefining (3) into the general form yields

$$g(t) \approx \sqrt{|k_0|} f(k_0 t - \tau_0), \quad (6)$$

where  $k_0 \approx 1 - \frac{2v}{c}$  if  $|v/c| \ll 1$  still holds [10]. The *Wideband Ambiguity Function* (WAF) [12] is derived as

$$WAF_{f,g}(k, \tau) = \sqrt{|k|} \int_{-\infty}^{\infty} f(kt - \tau) g^*(t) dt. \quad (7)$$

The WAF described in (7) is read as “scale first, then delay”. The auto WAF is considered a special case of the more general cross WAF and is denoted e.g.  $WAF_{f,f}$  or  $WAF_{g,g}$ .

For a finite, discrete signal, the continuous WAF can be approximated for a sufficiently long signal with sufficiently high sampling frequency. Nevertheless, the time scaling always require some form of interpolation.

## 2.4 I/Q Modulation

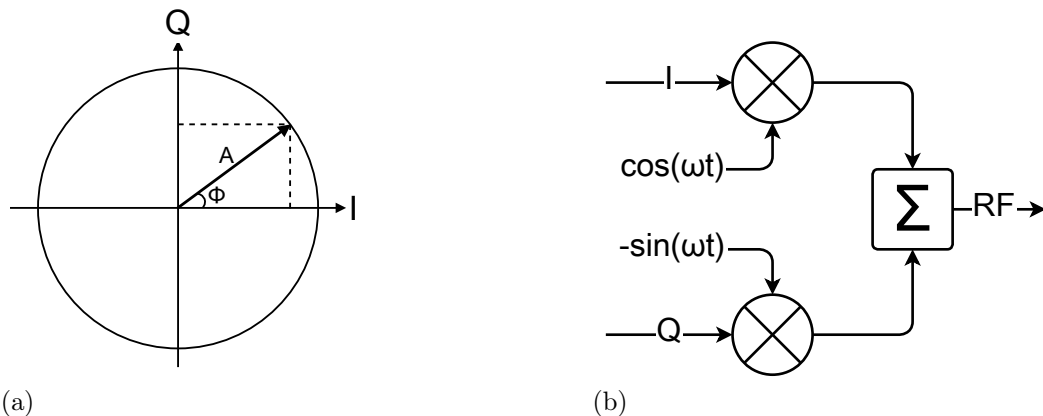


Figure 3: Illustrations of an I/Q vector and an overview of an I/Q modulator.



Issued by  
 John Dahl and Sebastian Holmqvist  
 Classification - Export Control  
 NOT EXPORT CONTROLLED

Date 2013-06-11 Issue A Document ID EX020/2013  
 Classification - Company Confidentiality  
 UNCLASSIFIED  
 Classification - Defence Secrecy  
 ÖPPEN/UNCLASSIFIED

I/Q modulation is currently one of the most common techniques used in signal processing. In practice, signals with rapidly changing amplitude/phase are difficult to generate accurately with a single oscillator source. With I/Q modulation, the amplitude and the phase of a signal are mixed from two separate oscillator sources. One being “in phase” and the other shifted by  $90^\circ$  and denoted “quadrature”.

As seen in Figure 3, an arbitrary complex baseband signal described in polar coordinates can be expressed by an angle  $\Phi$  and amplitude  $A$ . The I/Q modulation requires the signal to be divided into two parts, which is accomplished by mapping it into cartesian coordinates. The mapping between polar coordinates and cartesian coordinates is given by

$$\begin{cases} I = A \cos(\Phi) \\ Q = A \sin(\Phi). \end{cases} \quad (8)$$

The complex baseband signal,  $s(t)$ , is then formulated as

$$s(t) = I(t) + jQ(t), \quad (9)$$

where  $I(t)$  and  $Q(t)$  are orthogonal. By mixing the baseband signal onto a carrier wave, the reference signal,  $f(t)$ , is derived as

$$f(t) = s(t)e^{j\omega_c t}, \quad (10)$$

for a carrier wave angular frequency,  $\omega_c$ . Using Euler’s formula, (10) is expanded as

$$\begin{aligned} f(t) = & I(t) \cos(\omega_c t) + Q(t) \sin(\omega_c t) \\ & + jQ(t) \cos(\omega_c t) + jI(t) \sin(\omega_c t), \end{aligned} \quad (11)$$

with two real and two imaginary terms.

The imaginary parts of  $f(t)$  are inevitably omitted in a physical realization, e.g., the modulator overview in Figure (3). Using conjugate rules, (11) results in

$$\Re \{f(t)\} = I(t) \cos(\omega_c t) + Q(t) \sin(\omega_c t). \quad (12)$$



Issued by  
 John Dahl and Sebastian Holmqvist  
 Classification - Export Control  
 NOT EXPORT CONTROLLED

Date 2013-06-11 Issue A Document ID EX020/2013  
 Classification - Company Confidentiality  
 UNCLASSIFIED  
 Classification - Defence Secrecy  
 ÖPPEN/UNCLASSIFIED

Given that the reference signal is transmitted through a ideal channel without any additive distortions, the received signal,  $g(t)$ , is demodulated by multiplying (12) with the complex conjugate of the carrier wave, which yields

$$g(t)e^{-j\omega_c t} = \frac{1}{2}I(t)(1 + \cos(2\omega_c t) - j \sin(2\omega_c t)) + j\frac{1}{2}Q(t)(1 - \cos(2\omega_c t) - \sin(2\omega_c t)). \quad (13)$$

As given by (13), the demodulation causes even harmonics to arise which have to be suppressed by a lowpass filter in order to recreate the original baseband signal,  $s(t)$ . A drawback with filtering is that it also affects the desired part of the signal by introducing a gain and a phase delay. Introducing the *Hilbert Transform* (HT) allows for calculating the quadrature component directly from a real, in-phase signal, without any filtering needed.

The HT is defined as the convolution with the Hilbert transformer,  $1/\pi t$ . Formally, for an arbitrary signal  $f(t)$ , it is formulated as

$$F(s) = \mathcal{H}[f(t)] = \frac{1}{\pi}PV \int_{-\infty}^{\infty} \frac{f(t)}{t-s} dt, \quad (14)$$

and its inverse as

$$f(t) = \mathcal{H}^{-1}[F(s)] = -\frac{1}{\pi}PV \int_{-\infty}^{\infty} \frac{F(s)}{t-s} ds, \quad (15)$$

where the *Cauchy principal value*,  $PV$ , is taken in each of the integrals. The HT is linear, orthogonal to its real function and does not add nor remove any energy. Specifically, it can be shown that, for a strong analytical signal  $f(t)$ ,  $\mathcal{H}[\Re\{f(t)\}] = \Im\{f(t)\}$ . [3]

For a real, sampled signal as the one from (12), the complex I/Q signal,  $s(t) = I(t) + jQ(t)$ , can easily be retrieved by first applying the HT and then multiplying the result with the complex conjugated carrier frequency. Thus canceling the complex carrier wave.



Issued by  
John Dahl and Sebastian Holmqvist  
Classification - Export Control  
NOT EXPORT CONTROLLED

Date 2013-06-11 Issue A Document ID EX020/2013  
Classification - Company Confidentiality  
UNCLASSIFIED  
Classification - Defence Secrecy  
ÖPPEN/UNCLASSIFIED

## 3 Methodology

In this section, the measurement procedure is discussed in terms of the measuring rig, signal processing and validation.

The method serves to evaluate how the target detection is affected when passing a wideband signal through the PA, and how the PA affects SINR when matched against a pre-defined filter for a set of scenario optimal MIMO signals.

### 3.1 Measuring Rig

In order to generate and analyze arbitrary wideband signals, a comprehensive measuring rig was constructed. Below, the equipment and associated data file structure are outlined.

#### 3.1.1 Equipment

The measuring equipment, consisting mainly of a computer, a baseband generator, a signal generator, and an oscilloscope, were connected by a common communication bus, *General Purpose Interface Bus* (GPIB)<sup>1</sup> (see Figure 4). This setup allowed for the computer to act both as a data processing unit and as the GPIB controller, allowing for, e.g., automated measuring sequences and remote control.

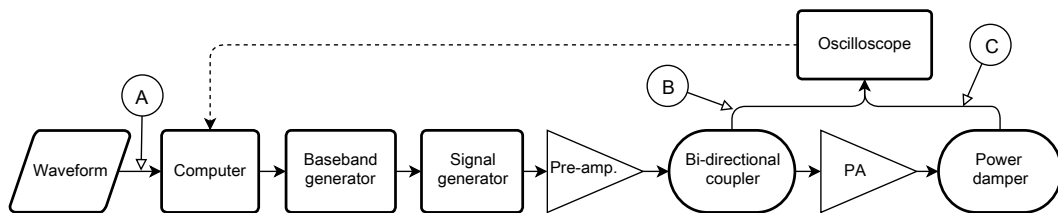


Figure 4: Hardware overview of the measuring rig with nodes I, II and III.

In order to ensure repeatability, the instruments were run at their specified operational temperature in a climate controlled lab. Before each measurement cycle, the instruments were reset and reconfigured, to ensure default settings

<sup>1</sup>GPIB is outlined in the IEEE 488-1975 standard and is commonly used in products from, e.g., TEKTRONIX, AGILENT, etc.



Issued by  
John Dahl and Sebastian Holmqvist  
Classification - Export Control  
NOT EXPORT CONTROLLED

Date 2013-06-11 Issue A Document ID EX020/2013  
Classification - Company Confidentiality  
UNCLASSIFIED  
Classification - Defence Secrecy  
ÖPPEN/UNCLASSIFIED

before each data set was processed. To maximize the resolution of the oscilloscope, the vertical scale was tuned to match each input power level. The time resolution was set to oversample the highest signal frequency to avoid aliasing.

### 3.1.2 File Structure

A date and label oriented file structure was created to manage and store data in an accessible order. To ensure that the stored data is retrievable, correct names, labels, and parameters were carefully set.

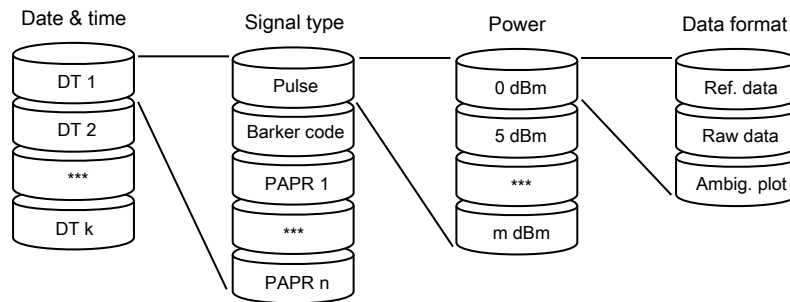


Figure 5: Schematic of the file structure.

Figure 5 describes the topology of the file structure, divided into four levels. The measurement data was stored in a descending order of date and time, signal type, input power used and finally the saved file type. For each data set, the input data was stored together with the raw data outputs and multiple image formats of the generated ambiguity plots.

### 3.2 Signal Processing

In any radar system, parameters such as power, range, target ambiguity, SINR, etc., are all collectively critical for the application. To measure how the PA affects the transmitted signal, the signal properties were evaluated before and after passing the PA.

As a reasonability check, the PA narrowband transfer function was derived using a network analyzer. The pre-amplifier allowed for the PA to be driven into compression (20 dBm), i.e., its operating point. In order to compensate



Issued by  
John Dahl and Sebastian Holmqvist  
Classification - Export Control  
NOT EXPORT CONTROLLED

Date                      Issue                      Document ID  
2013-06-11            A                              EX020/2013  
Classification - Company Confidentiality  
UNCLASSIFIED  
Classification - Defence Secrecy  
ÖPPEN/UNCLASSIFIED

---

for the pre-amplifier, both equipments were separately analyzed and the final transfer function was then calculated using MATLAB.

The WAF acts as a sensitivity analysis in Doppler and time delay, effectively describing the target ambiguity. From the sampled signals, before and after the PA (see Figure 4), both an  $WAF_{B,B}$  and an  $WAF_{B,C}$  were generated. The  $WAF_{B,B}$  served as a reference, and by comparison, the  $WAF_{B,C}$  visualized the effects on the target ambiguity caused by the PA.

As an analysis for the MIMO radar case, 3 partial signals from a scenario-optimized set of signals were processed separately through the PA before they were combined and matched against a pre-defined filter. By evaluating the complete set before and after the PA, the calculated SINR serves as a measure of how well the signal properties have been preserved. Each MIMO signal set was evaluated for three separate PAPR (1.2 dB, 3 dB, and 6 dB) realizations and for two different input power levels (10 dBm and 20 dBm). As the sampled signals were real, the HT was first applied and the signals were then extracted, via a FFT, directly from the signal spectrums in order to avoid any errors from downsampling.

### 3.3 Validation

The hardware was verified in multiple steps. First, the individual components were verified on individual basis by probing them with different signal waveforms, power levels, etc. Next, the PA was excluded from the setup, allowing both oscilloscope inputs to be properly balanced in power. Finally, as part of verifying the signal processing routines, a narrowband signal was transmitted through the rig and then post-processed. The results were then matched against known references, such as barker code and unmodulated pulse. Thus, verifying both the hardware and the signal processing, simultaneously. By using I/Q demodulation, the generated signal was matched and verified against the ideal one.

A sensitivity analysis was performed to ensure the correctness of the WAF. By separately simulating a nonlinear gain, phase distortion and applying a narrow bandpass filter on one of the sampled signals, the effects of a nonlinear PA were visually distinguishable in the WAF.



Issued by  
John Dahl and Sebastian Holmqvist  
Classification - Export Control  
NOT EXPORT CONTROLLED

Date                      Issue                      Document ID  
2013-06-11            A                              EX020/2013  
Classification - Company Confidentiality  
UNCLASSIFIED  
Classification - Defence Secrecy  
ÖPPEN/UNCLASSIFIED

---

## 4 Implementation

The lab setup, as seen in Figure 4, consisted of a TEKTRONIX AWG520 baseband generator, an AGILENT E4433B signal generator, a 24 dB gain pre-amplifier, a 20 dB bi-directional coupler, a 20 dB gain PA, a 40 dB power damper unit and a TEKTRONIX TDS7404 oscilloscope (see appendix A). A GPIB application layer was implemented in order to allow for direct instrument control from MATHWORKS MATLAB. A desktop PC was used as the GPIB controller and performed both the pre- and post-processing of the data.

As a part of validating the hardware setup, the PA baseline was established by the derivation of its narrowband transfer function. The PA was swept from 20 to 100 MHz, using a network analyzer, and the gain and phase was calculated at each frequency for a number of input power levels.

### 4.1 Measurement Analysis

As active devices are in general built from nonlinear components, they have the drawback of producing unwanted harmonics [2]. Harmonics appear in the power spectrum as multiples of the original frequencies and steal energy from the desired signal, which lowers the total *Signal to Noise Ratio* (SNR). The rig included, a part from the PA, four active devices: the baseband generator, the signal generator, the pre-amplifier, and the oscilloscope.

The TEKTRONIX AWG520 baseband generator converts a digital signal into its analog equivalent, using a 10 bit *Digital to Analog Converter* (DAC). The TEKTRONIX TDS7404 oscilloscope acquires data and uses an 8 bit *Analog to Digital Converter* (ADC) to convert an analog signal into a digital signal. An ADC is often a source of harmonics, due to the inability to describe each sample value exactly. This inherent flaw is referred to as *quantization noise*, denoted  $SNR_Q$ .

The  $SNR_Q$  is usually linearly dependent on the number of bits in the ADC [8]. However, if the signal noise level is larger than the *Least Significant Bit* (LSB), the *Effective Number of Bits* (ENOB) possible is reduced, which in turn lowers the  $SNR_Q$ . The  $SNR_Q$  is defined as

$$SNR_Q = 6.02 \cdot ENOB + 1.76 \quad (16)$$

As the baseband generator only has a DAC, it equals to 10 ENOB. The oscilloscope has a 8 bit ADC but only performs at 5.6 ENOB under said condi-



Issued by  
John Dahl and Sebastian Holmqvist  
Classification - Export Control  
NOT EXPORT CONTROLLED

Date 2013-06-11 Issue A Document ID EX020/2013  
Classification - Company Confidentiality  
UNCLASSIFIED  
Classification - Defence Secrecy  
ÖPPEN/UNCLASSIFIED

---

tions, which yields a  $SNR_Q$  of 62.0 dB and 35.5 dB, respectively. Thus, from a quantization noise perspective, the weakest link in the rig was the oscilloscope.

Sample clock jitter is another common source of noise described in (17) where  $\Delta t$  is the jitter standard deviation in seconds and  $f_{max}$  is the maximum frequency from the signal [1].

$$SNR_J = -20 \cdot \log_{10} (\Delta t \cdot 2\pi \cdot f_{max}) \quad (17)$$

The jitter of the baseband generator has a standard deviation of 11 ps and the oscilloscope has a standard deviation of 1.15 ps. Insertion into (17) yields a  $SNR_J$  of 45.7 and 63.0 dB, respectively. In total, the sum of all SNR values was calculated to 35.1 dB, just below the quantization noise. Thus, the oscilloscope had the weakest SNR, which made it crucial to select the vertical range of the oscilloscope to match the power level in use.

The AGILENT E4433B signal generator has a built in arbitrary baseband generator that can process digital I/Q samples with a theoretical bandwidth of 40 MHz. However, in practice, with acceptable level of accuracy, it could not perform better than 10 MHz. To be classified as *ultra wideband*, the fractional bandwidth,  $B = f_B/f_c$ , where  $f_B$  is the bandwidth and  $f_c$  is the center frequency, must exceed 20%. Even if a 10 MHz bandwidth and a carrier frequency of 50 MHz satisfies the criterion of ultra wideband signals, a larger bandwidth was desired. Therefore, an external TEKTRONIX AWG510 baseband generator was used, which generates analog I/Q data in separate channels. The AGILENT signal generator then mixes both the channels and applies the carrier frequency. This setup enabled a practical I/Q update frequency of 50 MHz, which was considered wideband enough. A drawback with this cascade coupling is that the mixing is not ideal and this could be seen as spectral power leakage from the carrier frequency, which affected the post processing.

In order to ensure repeatability, temperature control/measurement is another important factor. In a practical application, temperature control normally consists of transporting as much of the excess heat away from the amplifier as possible. As a typical application has a duty factor of 5–10 % of the total time, it means that basically all transmissions originate from an idle/stationary temperature. Ideally, a sensitivity analysis would establish the connection



Issued by  
 John Dahl and Sebastian Holmqvist  
 Classification - Export Control  
**NOT EXPORT CONTROLLED**

Date 2013-06-11 Issue A Document ID EX020/2013  
 Classification - Company Confidentiality  
**UNCLASSIFIED**  
 Classification - Defence Secrecy  
**ÖPPEN/UNCLASSIFIED**

between temperature and linearity. In this study however, the temperature variation was determined negligible.

To make sure that a correct power level feeds the PA, the combined output power from the baseband generator, the signal generator, and the pre-amplifier were measured with a HP 437B power meter. Several narrowband signals (e.g., sine, unmodulated pulse, barker code) and PAPR optimized wideband signals were used to validate that the actual output power matched the desired one. The deviation between measured and desired power was below 0.5 dBm.

### 4.2 Signal Analysis

Each signal passed through three stages: pre-processing, signal process and post-processing. An overview of the entire process is illustrated in Figure 6.

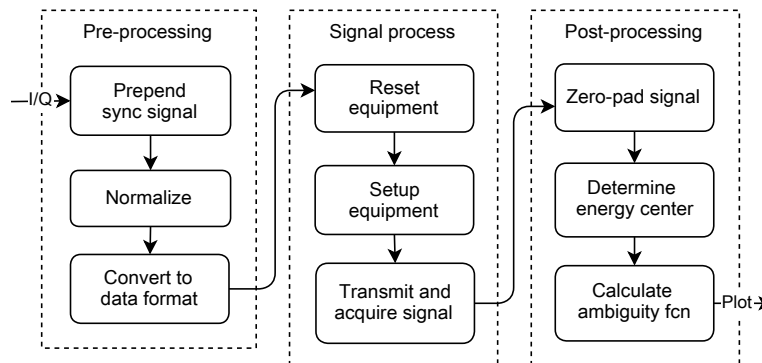


Figure 6: Overview of the three stage signal flow.

#### 4.2.1 Pre-processing

A minimal signal sample length ensures that a sufficiently large part of the carrier wave is included in the sampled signal. If the signal was shorter than desired, it was reconstructed using a *Zero Order Hold* (ZOH) to an upsampled, proper, sample length before being pre-processed. In order to detect the phase of the carrier wave in post-processing, a 10 sample sync signal was generated and prepended to the signal. Finally, the signal was normalized according to  $\max_n \left( \sqrt{I_n^2 + Q_n^2} \right) = 1$ , before being converted to a compatible *uint16* data format.



Issued by  
John Dahl and Sebastian Holmqvist  
Classification - Export Control  
NOT EXPORT CONTROLLED

Date                      Issue                      Document ID  
2013-06-11              A                              EX020/2013  
Classification - Company Confidentiality  
UNCLASSIFIED  
Classification - Defence Secrecy  
ÖPPEN/UNCLASSIFIED

---

## 4.2.2 Signal Process

After the pre-processing stage, the equipment was reset to its factory defaults. The AGILENT signal generator was configured to mix the I/Q input from the TEKTRONIX baseband generator, with a I/Q update frequency,  $f_m$ , onto a carrier wave frequency,  $f_c$ . Next, the TEKTRONIX oscilloscope was configured to sample the signal with a sampling frequency,  $f_s$ , both before and after the PA (see Figure 4). The TEKTRONIX generator was then initialized by a trigger event and the resulting signal was sampled. Finally, the sampled data was transferred over GPIB to the computer, converted and truncated to an appropriate signal length.

## 4.2.3 Post-processing

In order to validate the generated signal, prior passing the PA, the signal was sampled and then, using the HT, converted back to complex form. The sync signal was then used to determine the phase of the carrier wave, and any offset caused by the triggering. The signal was then demodulated using the complex conjugate of the carrier wave. Using bi-directional filtering, in order to allow zero-phase filtering [5], a Butterworth filter was finally applied to attenuate any aliasing caused by the demodulation.

Before calculating the WAF, the raw sampled signals were first zero-padded in order to avoid any loss of energy. Then, in order to avoid skewing, the time vectors were centered around the signals energy centers.

## 4.2.4 WAF Implementation

The implementation of the WAF differs from the NAF implementation as time scaling is employed instead of a narrowband frequency shift. To calculate the WAF of two raw, sampled, signals  $SIG1$  and  $SIG2$ , the algorithm boils down to the following steps:

1. Hilbert transform  $SIG1$  and  $SIG2$  to analytic, complex, signals.
2. Transform  $SIG1$  to a N point FFT signal ( $SIG1\_FFT$ ).
3. Complex conjugate  $SIG1\_FFT$  ( $SIG1\_CONJ$ ).
4. For each Doppler scaling:
  - (a) Time scale  $SIG2$  using linear interpolation ( $SIG2\_INT$ ).



Issued by  
John Dahl and Sebastian Holmqvist  
Classification - Export Control  
NOT EXPORT CONTROLLED

Date 2013-06-11 Issue A Document ID EX020/2013  
Classification - Company Confidentiality  
UNCLASSIFIED  
Classification - Defence Secrecy  
ÖPPEN/UNCLASSIFIED

---

- (b) Transform  $SIG2\_INT$  to a N point FFT signal ( $SIG2\_FFT$ ).
  - (c) Multiply  $SIG1\_CONJ$  and  $SIG2\_FFT$  element-wise and transform back using IFFT.
  - (d) Extract the relevant number of time lags and save to a matrix ( $WAF\_MAT$ ).
5. Normalize the resulting  $WAF\_MAT$ .
  6. Convert to dB and truncate, for example, below -35 dB.
  7. Decimate and plot results.

For a pre-defined number of phase rotations of the carrier wave, the Doppler scaling factor,  $k$ , was calculated using:

$$\frac{f_c}{f_c + \frac{M}{\tau_0}} \leq k \leq \frac{f_c}{f_c - \frac{M}{\tau_0}}, \quad (18)$$

where  $M$  represents the number of phase rotations and  $\tau_0$  is the nominal signal time duration.



Issued by  
John Dahl and Sebastian Holmqvist  
Classification - Export Control  
**NOT EXPORT CONTROLLED**

Date 2013-06-11 Issue A Document ID EX020/2013  
Classification - Company Confidentiality  
**UNCLASSIFIED**  
Classification - Defence Secrecy  
**ÖPPEN/UNCLASSIFIED**

## 5 Results

In this section, the results from the narrowband analysis, target ambiguity and its validation are presented for a representative A-B class PA.

### 5.1 Narrowband Linearity

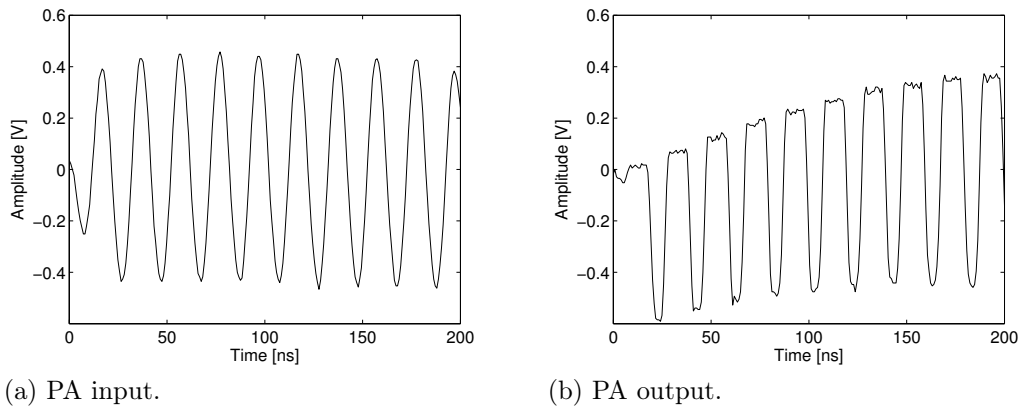


Figure 7: PA sinusoid sampled from node B and C.

A 50 MHz sinusoid is sampled before and after the PA and plotted in Figure 7 to visualize the distortion produced by the PA. Note the initial transient behavior and the positive single side saturation of the output sinusoid.



Issued by  
John Dahl and Sebastian Holmqvist  
Classification - Export Control  
**NOT EXPORT CONTROLLED**

Date 2013-06-11 Issue A Document ID EX020/2013  
Classification - Company Confidentiality  
**UNCLASSIFIED**  
Classification - Defence Secrecy  
**ÖPPEN/UNCLASSIFIED**

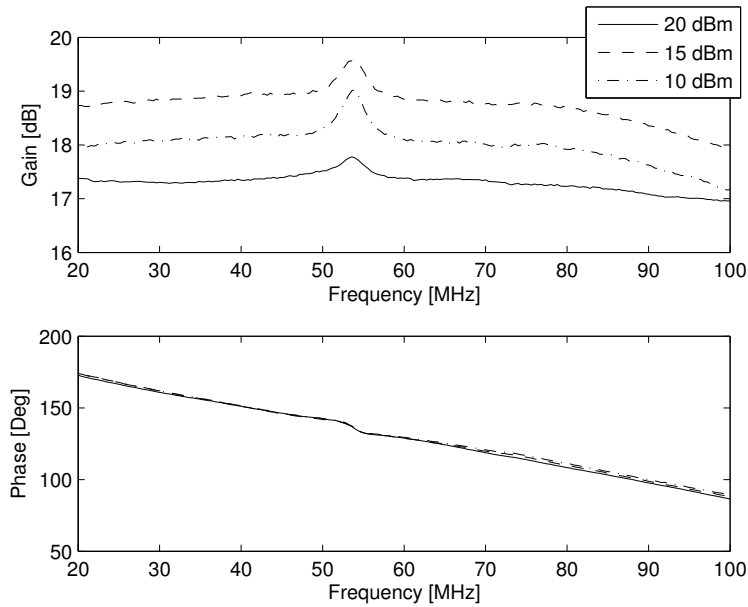


Figure 8: The gain and phase transfer function for the PA as a function of input power.

The narrowband PA specific gain and phase transfer function can be seen in Figure 8. Note how the PA gain is clearly depending on input power. The phase is however independent of the input power. Below the compression point at 18 dBm, an increase in input power yields a larger PA gain. Above the compression point, the PA gain decreases as the input power increases. The gain is fairly smooth, and without sharp notches or ripple. At 50–55 MHz, a gain “bulge” of approximately 1 dB is visible.



Issued by  
John Dahl and Sebastian Holmqvist  
Classification - Export Control  
**NOT EXPORT CONTROLLED**

Date 2013-06-11 Issue A Document ID EX020/2013  
Classification - Company Confidentiality  
**UNCLASSIFIED**  
Classification - Defence Secrecy  
**ÖPPEN/UNCLASSIFIED**

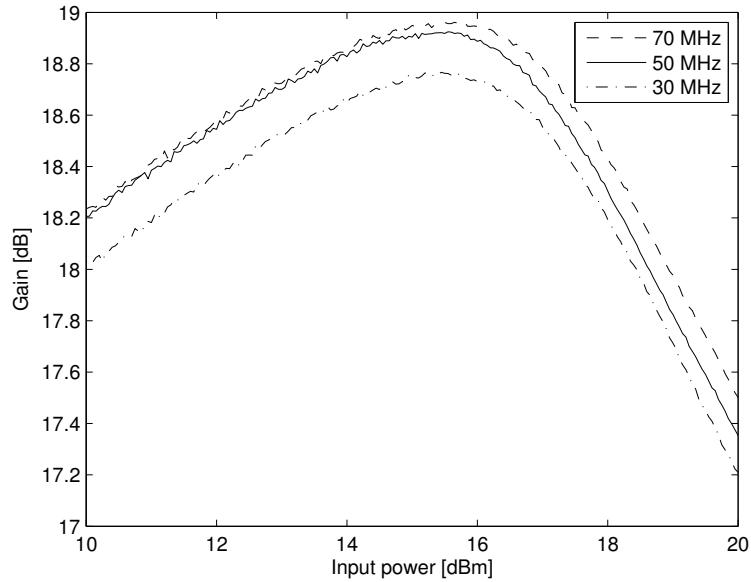


Figure 9: The PA gain as a function of input power.

The nonlinear relation between input power (node B) and the corresponding gain is represented in Figure 9. The gain increases linearly for low input powers but decreases for large input powers. At approximately 15 dBm, i.e., the local maximum of the gain, the decrease in gain indicates the lower bound of input power required to drive the PA into compression.



Issued by  
John Dahl and Sebastian Holmqvist  
Classification - Export Control  
NOT EXPORT CONTROLLED

Date 2013-06-11 Issue A Document ID EX020/2013  
Classification - Company Confidentiality  
UNCLASSIFIED  
Classification - Defence Secrecy  
ÖPPEN/UNCLASSIFIED

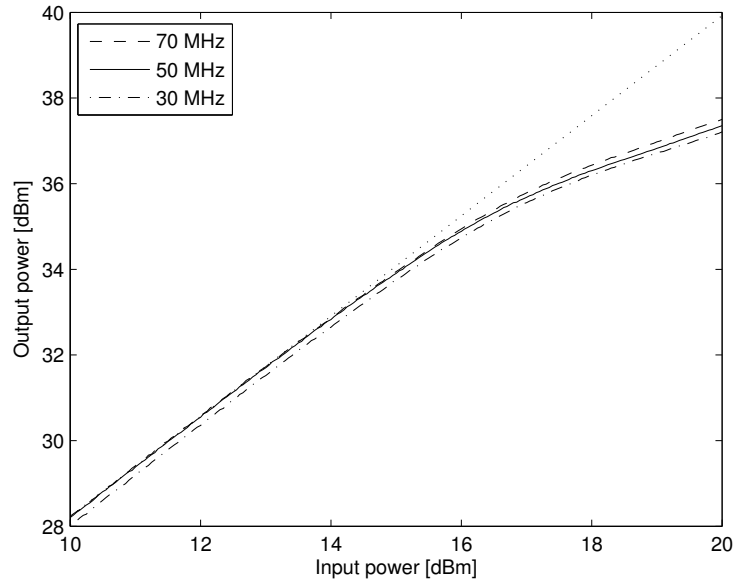


Figure 10: The PA output power as a function of input power.

The ratio between input and output power is shown in Figure 10. The PA is linearly increasing for small input powers but starts declining for larger input powers. The 1 dB compression point occurs at approximately 18 dBm input power.

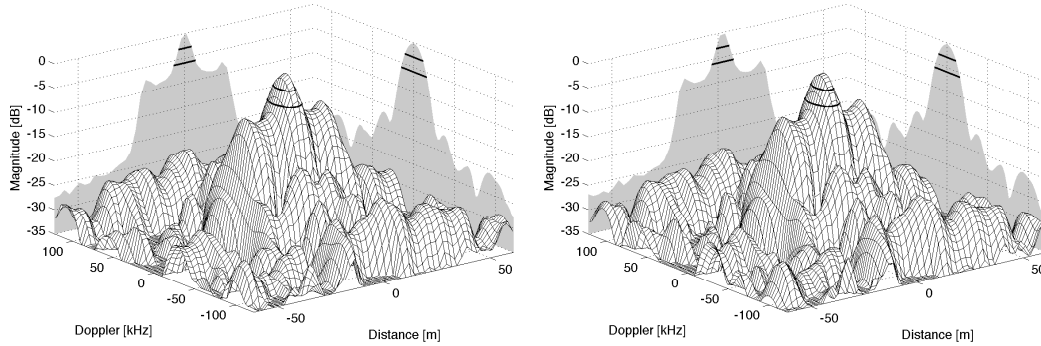
## 5.2 Target Ambiguity

A signal aimed for a MIMO radar system is processed at 10 and 20 dBm input power, i.e., below and above the 1 dB compression point. The  $WAF_{B,B}$  is first plotted and used as reference, and then the  $WAF_{B,C}$  is plotted and compared to the  $WAF_{B,B}$  reference. All plots are normalized and presented in logarithmic scale. As the results are identical, only the 20 dBm figure are displayed below.



Issued by  
 John Dahl and Sebastian Holmqvist  
 Classification - Export Control  
 NOT EXPORT CONTROLLED

Date 2013-06-11 Issue A Document ID EX020/2013  
 Classification - Company Confidentiality  
 UNCLASSIFIED  
 Classification - Defence Secrecy  
 ÖPPEN/UNCLASSIFIED

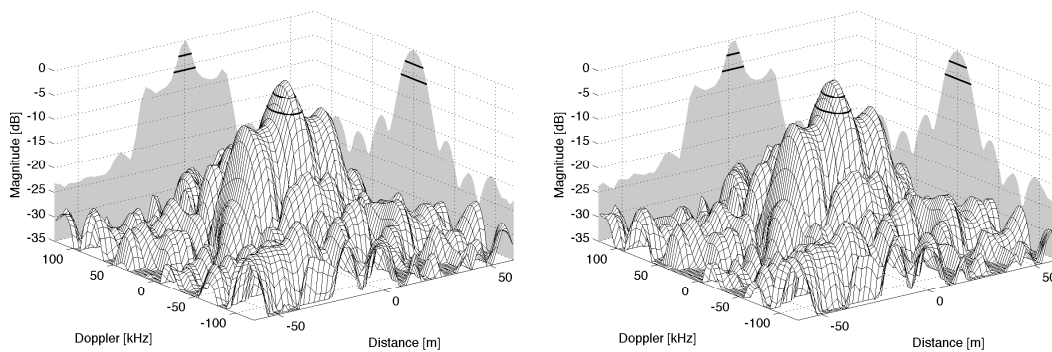


(a)  $WAF_{B,B}$ .

(b)  $WAF_{B,C}$ .

Figure 11: WAF plots of a single MIMO set signal with a PAPR of 1.2 dB at input power 20 dBm.

In Figure 11, the  $WAF_{B,B}$  and  $WAF_{B,C}$  plots depicts a single signal from a set of MIMO signals at 1.2 dB PAPR. The reference  $WAF_{B,B}$  has two shoulders at approximately -8 dB, and a perceived side lobe level around -25 to -20 dB. The  $WAF_{B,C}$  is strikingly similar with a small offset in distance causing the main lobe to shift slightly.



(a)  $WAF_{B,B}$ .

(b)  $WAF_{B,C}$ .

Figure 12: WAF plots of a single MIMO set signal with a PAPR of 3 dB at input power 20 dBm.

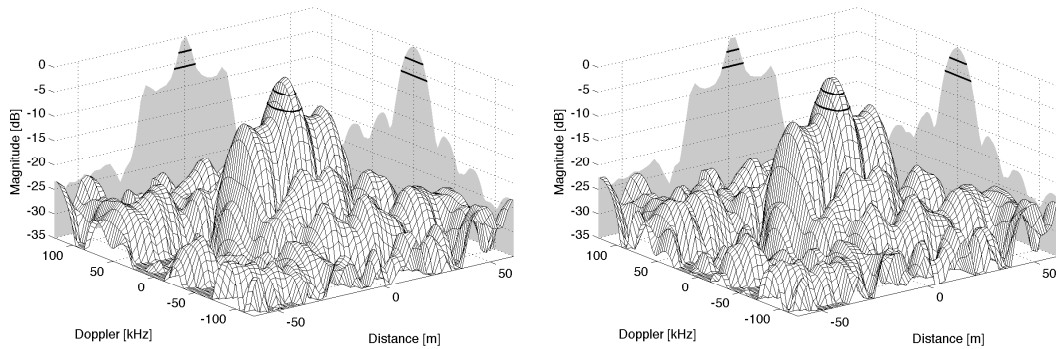
For a signal with 3 dB PAPR, the  $WAF_{B,B}$  and the  $WAF_{B,C}$  are illustrated



Issued by  
John Dahl and Sebastian Holmqvist  
Classification - Export Control  
NOT EXPORT CONTROLLED

Date 2013-06-11 Issue A Document ID EX020/2013  
Classification - Company Confidentiality  
UNCLASSIFIED  
Classification - Defence Secrecy  
ÖPPEN/UNCLASSIFIED

in Figure 12. Similar to the 1.2 dB signal, the  $WAF_{B,C}$  barely differs from the  $WAF_{B,B}$ .



(a)  $WAF_{B,B}$ .

(b)  $WAF_{B,C}$ .

Figure 13: WAF plots of a single MIMO set signal with a PAPR of 6 dB at input power 20 dBm.

Finally, at 6 dB PAPR, the signal is processed and plotted in Figure 13. Once again, the  $WAF_{B,B}$  and  $WAF_{B,C}$  are strikingly similar.



Issued by  
 John Dahl and Sebastian Holmqvist  
 Classification - Export Control  
 NOT EXPORT CONTROLLED

Date 2013-06-11 Issue A Document ID EX020/2013  
 Classification - Company Confidentiality  
 UNCLASSIFIED  
 Classification - Defence Secrecy  
 ÖPPEN/UNCLASSIFIED

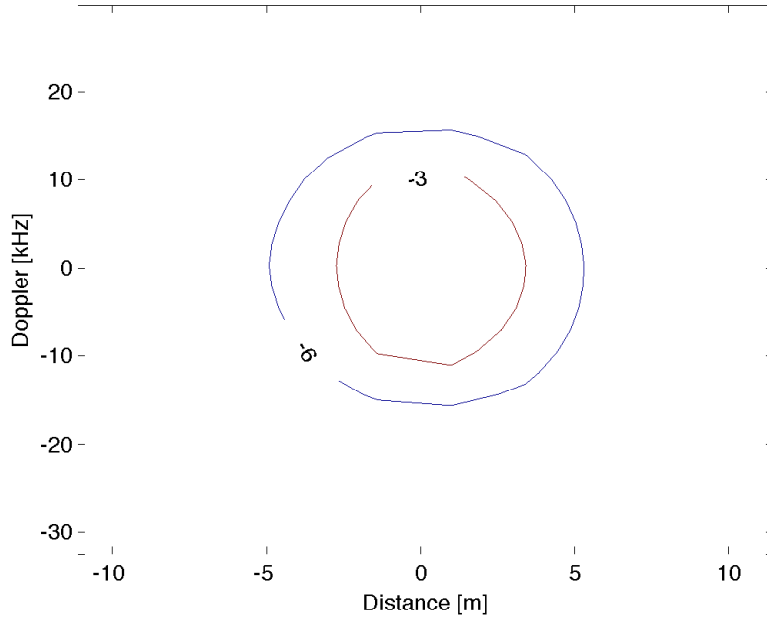


Figure 14: Contour plot with -3 and -6 dB nodes of a 1.2 dB PAPR signal at input power 20 dBm.

As a qualitative measurement, the -3 and -6 dB cross-sections are measured in the Doppler and distance axes. As can be seen in Figure 14, the ellipsoid shapes of the contours are closely aligned with the axes of the figure.

	Distance [m]		Doppler [kHz]	
	-3 dB	-6 dB	-3 dB	-6 dB
$WAF_{B,B}$	6.2	10.2	21.5	31.0
$WAF_{B,C}$	6.1	10.3	21.5	31.4
Diff. [%]	1.6	-1.0	0.0	-1.3

Table 1: Cross-section measurements for a 1.2 dB PAPR signal at input power 20 dBm.



Issued by  
 John Dahl and Sebastian Holmqvist  
 Classification - Export Control  
 NOT EXPORT CONTROLLED

Date 2013-06-11 Issue A Document ID EX020/2013  
 Classification - Company Confidentiality  
 UNCLASSIFIED  
 Classification - Defence Secrecy  
 ÖPPEN/UNCLASSIFIED

	Distance [m]		Doppler [kHz]	
	-3 dB	-6 dB	-3 dB	-6 dB
$WAF_{B,B}$	6.1	10.3	21.5	31.3
$WAF_{B,C}$	6.2	10.5	21.8	31.6
Diff. [%]	-1.6	-1.9	-1.4	-1.0

Table 2: Cross-section measurements for a 3 dB PAPR signal at input power 20 dBm.

	Distance [m]		Doppler [kHz]	
	-3 dB	-6 dB	-3 dB	-6 dB
$WAF_{B,B}$	6.0	10.0	22.0	31.8
$WAF_{B,C}$	6.0	10.1	21.8	31.7
Diff. [%]	0.0	-1.0	0.9	0.3

Table 3: Cross-section measurements for a 6 dB PAPR signal at input power 20 dBm.

Table 1, 2 and 3 shows a maximum absolute deviation of 1.9%. As mentioned earlier, the  $WAF_{B,B}$  and the  $WAF_{B,C}$  plots are strikingly similar.

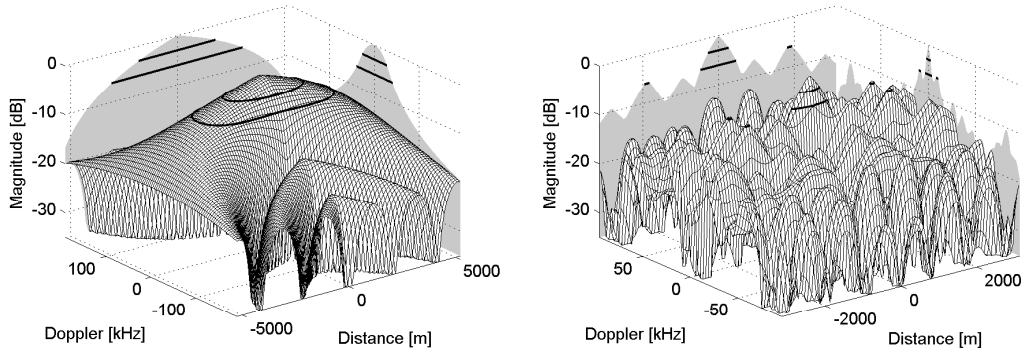
### 5.3 WAF Validation

Initially, the WAF implementation is validated by comparing plots of to known references. Next, the WAF is plotted for several simulated signal distortions, emulating a PA.



Issued by  
 John Dahl and Sebastian Holmqvist  
 Classification - Export Control  
**NOT EXPORT CONTROLLED**

Date 2013-06-11 Issue A Document ID EX020/2013  
 Classification - Company Confidentiality  
**UNCLASSIFIED**  
 Classification - Defence Secrecy  
**ÖPPEN/UNCLASSIFIED**



(a) Unmodulated pulse.

(b) Barker 13 code.

Figure 15:  $WAF_{A,A}$  plots of an unmodulated pulse and Barker code signal.

Figure 15 displays  $WAF_{A,A}$  plots of both an unmodulated pulse and Barker 13 code signal, which are used to verify the WAF against known implementations.

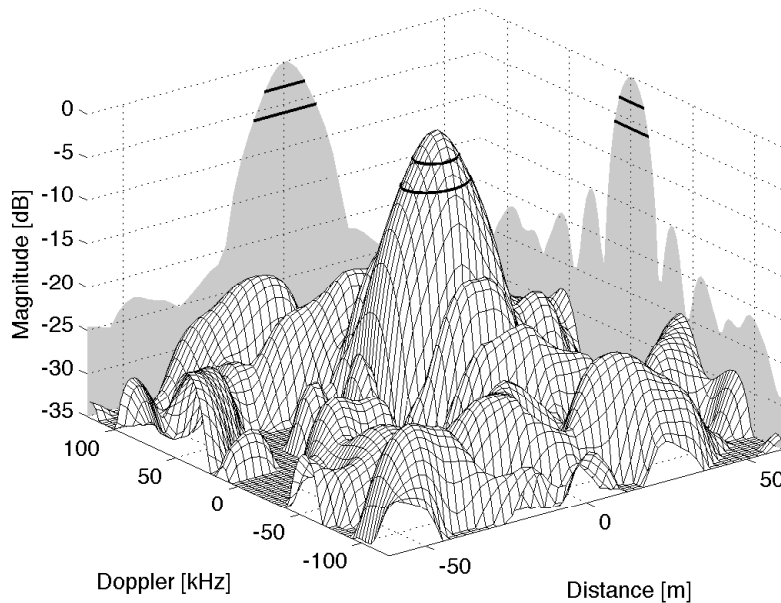


Figure 16:  $WAF_{B,B}$  plot from a single MIMO set signal provided as a reference.

This document and the information contained herein is the property of Saab AB and must not be used, disclosed or altered without Saab AB prior written consent.



Issued by  
John Dahl and Sebastian Holmqvist  
Classification - Export Control  
NOT EXPORT CONTROLLED

Date 2013-06-11 Issue A Document ID EX020/2013  
Classification - Company Confidentiality  
UNCLASSIFIED  
Classification - Defence Secrecy  
ÖPPEN/UNCLASSIFIED

A reference  $WAF_{B,B}$  plot is displayed in Figure 16. The processed signal is an example from a set of MIMO signals and is sampled at node B.

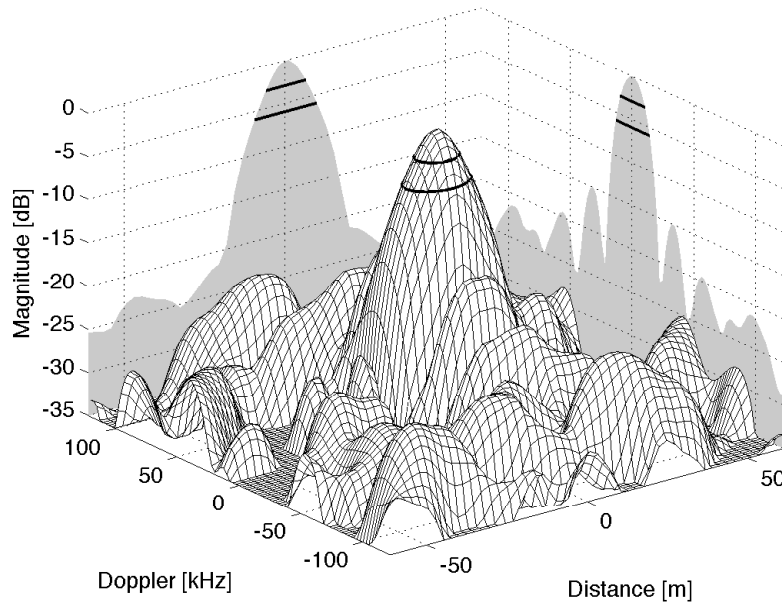


Figure 17:  $WAF_{B,C}$  plot with a simulated nonlinear gain.

In Figure 17, the  $WAF_{B,C}$  is plotted for a signal with a simulated nonlinear gain. A sampled reference signal is duplicated and saturated at 50 % before the  $WAF_{B,C}$  is calculated. Note how the  $WAF_{B,C}$  is visibly unaffected by the nonlinear saturation. The signal manipulation is made in the preprocessing stage, and the realized reference signal from node B is used as the base signal.



Issued by  
John Dahl and Sebastian Holmqvist  
Classification - Export Control  
**NOT EXPORT CONTROLLED**

Date 2013-06-11 Issue A Document ID EX020/2013  
Classification - Company Confidentiality  
**UNCLASSIFIED**  
Classification - Defence Secrecy  
**ÖPPEN/UNCLASSIFIED**

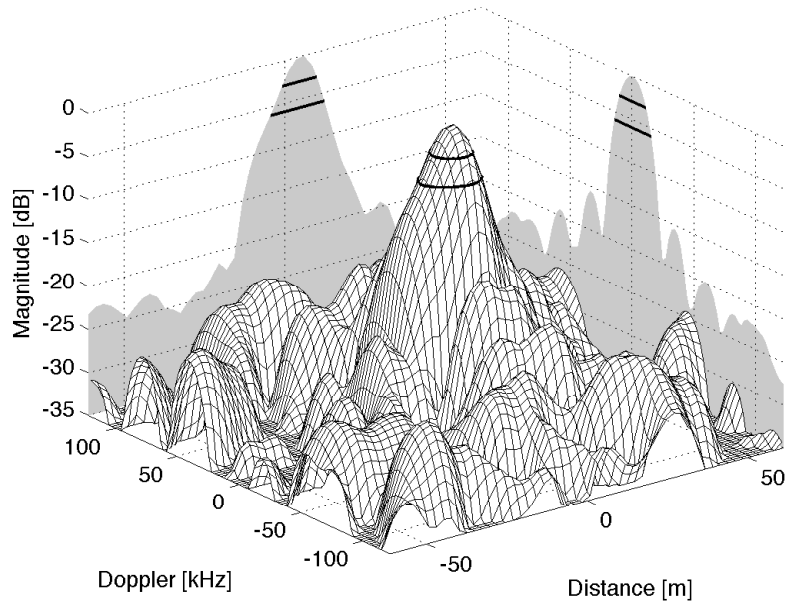


Figure 18:  $WAF_{B,C}$  plot with a simulated phase distortion.

For a 4th order Butterworth filter with a cutoff frequency,  $\omega_c = 100$  MHz, a replicate of the signal is convoluted with the filter causing a phase distortion. The  $WAF_{B,C}$  can be seen in Figure 18. Note the asymmetry introduced on the main lobe.



Issued by  
John Dahl and Sebastian Holmqvist  
Classification - Export Control  
NOT EXPORT CONTROLLED

Date 2013-06-11 Issue A Document ID EX020/2013  
Classification - Company Confidentiality  
UNCLASSIFIED  
Classification - Defence Secrecy  
ÖPPEN/UNCLASSIFIED

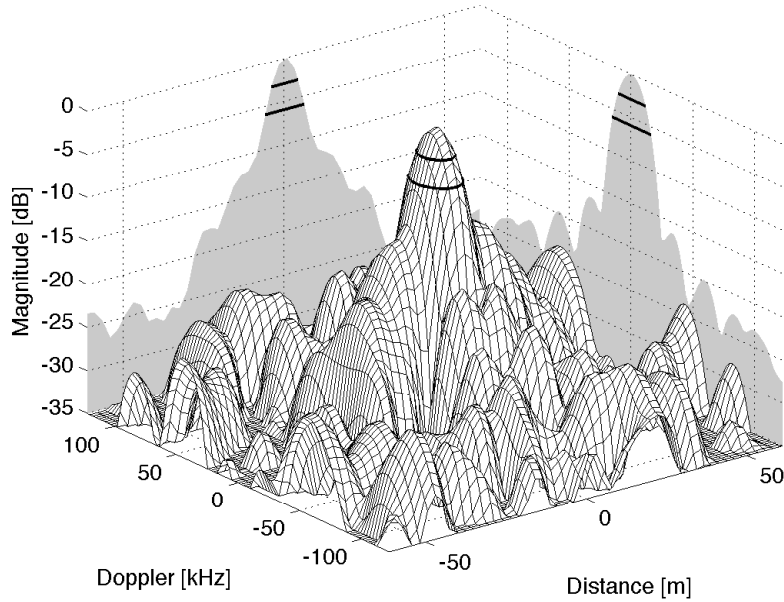


Figure 19:  $WAF_{B,C}$  plot with a simulated bandpass filter.

Finally, a sampled signal from node B is duplicated and convolved by a 2nd order bi-directional, zero-phase, Butterworth bandpass filter (30–70 MHz). The  $WAF_{B,C}$  and its introduced main lobe “shoulders” can be seen in Figure 19.

### 5.4 MIMO Analysis

A set of three different MIMO signals are processed and benchmarked against a pre-defined filter. The set of MIMO signals is optimized against one specific scenario, at three different PAPR levels.

Power	Ideal [dB]	$PA_{in}$ [dB]	$PA_{out}$ [dB]	$PA_{out-in}$ [dB]
10 dBm	20.04	16.07	4.50	-11.57
20 dBm	20.04	16.09	4.06	-12.03

Table 4: Calculated SINR for an optimal set of MIMO signals at 1.2 dB PAPR.



Issued by  
 John Dahl and Sebastian Holmqvist  
 Classification - Export Control  
 NOT EXPORT CONTROLLED

Date                      Issue                      Document ID  
 2013-06-11      A                      EX020/2013  
 Classification - Company Confidentiality  
 UNCLASSIFIED  
 Classification - Defence Secrecy  
 ÖPPEN/UNCLASSIFIED

Table 4 reveals a -4.0 dB decrease in SINR for the generated signal at 1.2 dB PAPR. The main drop of -12.0 dB is caused by the PA. The drop is slightly greater for the larger, 20 dBm, input power.

Power	Ideal [dB]	$PA_{in}$ [dB]	$PA_{out}$ [dB]	$PA_{out-in}$ [dB]
10 dBm	19.92	15.67	2.94	-12.73
20 dBm	19.92	15.48	2.42	-13.06

Table 5: Calculated SINR for an optimal set of MIMO signals at 3 dB PAPR.

For the signal in Table 5, realized at 3 dB PAPR, the initial decrease is now at -4.4 dB. The PA causes a -13.1 dB drop in SINR. The drop is slightly greater for the larger, 20 dBm, input power.

Power	Ideal [dB]	$PA_{in}$ [dB]	$PA_{out}$ [dB]	$PA_{out-in}$ [dB]
10 dBm	20.21	6.04	-3.67	-9.67
20 dBm	20.21	5.78	-4.53	-10.31

Table 6: Calculated SINR for an optimal set of MIMO signals at 6 dB PAPR.

The final signal, at 6 dB PAPR, causes issues with the measuring rig. As can be seen in Table 6, the SINR drops by as much as -14.4 dB for the generated, sampled, signal. The PA causes an additional drop of -10.3 dB. The drop is slightly greater for the larger, 20 dBm, input power.



Issued by  
John Dahl and Sebastian Holmqvist  
Classification - Export Control  
NOT EXPORT CONTROLLED

Date                      Issue                      Document ID  
2013-06-11            A                              EX020/2013  
Classification - Company Confidentiality  
UNCLASSIFIED  
Classification - Defence Secrecy  
ÖPPEN/UNCLASSIFIED

---

## 6 Analysis

In this section, the narrowband, ambiguity, and MIMO results are analyzed and discussed.

### 6.1 Narrowband

By looking at the envelope of the signals in Figure 7, it is clear that the PA has added distortion to the output signal. The positive part of the output signal has been single side saturated in comparison to the signal before the PA, and the saturation level seems proportional to the applied input power. This saturation is a natural consequence of the type A-B PA, since the power amplifier circuit is built upon a single biased transistor. The output signal is more distorted than the input signal, which is expected as all types of PA adds nonlinear distortion. These distortions are seen in the spectral domain as harmonics.

In a narrowband analysis perspective, with the PA dynamics in focus, it can be seen from Figure 8 that the gain is dependent on the input power and that the gain curves are almost flat over all frequencies. The PA is specified to run at 20 dBm input power and is driven into compression at 18 dBm input power. The dependency on input power is characteristic for an A-B amplifier, which rely on the stage current applied.

The phase is independent of input power and decreases constantly with 10° per decade. The phase data is compensated for equivalent cable length, which means that the additional phase delay related to the trace length of the PA circuit is canceled out. The relationship between equivalent trace length and phase delay is given by

$$\phi = \frac{2\pi}{\lambda} \cdot \frac{\ell}{\beta}, \quad (19)$$

where the wavelength is defined as  $\lambda = \frac{c}{f}$ ,  $c$  is the propagation speed of light,  $f$  is the signal frequency,  $\ell$  is the equivalent trace length and finally,  $\beta$  is the propagation constant. In this case,  $\ell$  and  $\beta$  are approximated to 0.2 m and 0.6 rad/m, respectively. Differentiating (19) with respect to the frequency gives the linear rate of phase delay in relation to the applied frequency, see (20).



Issued by  
John Dahl and Sebastian Holmqvist  
Classification - Export Control  
NOT EXPORT CONTROLLED

Date 2013-06-11 Issue A Document ID EX020/2013  
Classification - Company Confidentiality  
UNCLASSIFIED  
Classification - Defence Secrecy  
ÖPPEN/UNCLASSIFIED

---

$$\frac{\partial \phi}{\partial f} = \frac{2\pi}{c} \cdot \frac{\ell}{\beta} \quad (20)$$

The equivalent trace length of 0.2 m, yields a rate of phase delay equal to  $0.4^\circ/\text{MHz}$ . For example, a 100 MHz signal without equivalent trace length compensation would have a phase offset of  $40^\circ$ . In the range of 50–55 MHz, a small variation in phase can be seen, which corresponds to the bulge in the gain plot. This bulge is inherited from the PA development and has nothing to do with the measurement.

## 6.2 Ambiguity

The auto and cross WAF plots from the result section have some crucial properties in common – they are not sensitive to the level of PAPR nor the input power level. This means that despite all disturbances mentioned earlier, the ambiguity function is basically unaffected.

The ambiguity function is based on correlation, which is more sensitive to phase disturbances than magnitude disturbances. The robustness seen in the ambiguity functions indicates that the phase is not affected by the PA, which agrees with the narrowband results.

Time delay, in practice shifted samples, is closely linked to the sample rate of the acquired signal and is therefore easy to relate to the physical properties of time/distance. For frequencies below 100 MHz, the Doppler time shift is no longer trivial to relate to physical velocities as  $s \approx 1 - \frac{2v}{c}$  and  $v \ll c$ . A short pulse length is normally compensated by a long integration time, including several pulses, which scales the Doppler axis in the WAF. However, a long integration time yields a large number of data samples. Since the post-processing CPU is a 32-bit core, it is impractical to process that large vector. Instead, the Doppler scale in the ambiguity plots is calculated for very large velocities to ensure that the attenuation and sidelobes along the Doppler axis are visually included.

From a RADAR perspective, the robust and insensitive behavior of the ambiguity function is desirable, but to determine the amount of signal manipulation caused by the PA, it is not detailed enough.



Issued by  
John Dahl and Sebastian Holmqvist  
Classification - Export Control  
NOT EXPORT CONTROLLED

Date                      Issue                      Document ID  
2013-06-11              A                              EX020/2013  
Classification - Company Confidentiality  
UNCLASSIFIED  
Classification - Defence Secrecy  
ÖPPEN/UNCLASSIFIED

---

### 6.3 MIMO

The MIMO perspective analysis is more sensitive in respect to signal disturbance, than the ambiguity function. A sensible analysis method demands accurate input data, which in this case implies perfectly adjusted hardware, and input signals that are not too challenging on the hardware.

Using a signal with a PAPR of 1.2 dB yields a SINR loss of 4 dB after realization, and a loss of 11–12 dB after the PA. The drop of SINR is not connected to the input power level. The realization losses are a consequence of the oscilloscope's quantization noise, and limited bandwidth in the baseband generator. The losses over the PA originates from the signal saturation mentioned earlier, which level was declared proportional to the input power. This proportional saturation explains the SINR's independency of input power.

The 3 dB PAPR signal has slightly lower SINR than the 1.2 dB one, both after realization and after PA losses. This is because the envelope of the 3 dB signal is fluctuating more than the envelope of the 1.2 dB signal, which challenges the hardware further. Similarly, the 6 dB PAPR has really low SINR, which once again depicts the hardware's inability of realize signals containing large transients.

While a low PAPR signal requires computing power in order to be produced, the benefits of a constant power envelope are many. As PAPR goes towards 0 dB, the average power is maximized, and the detection range of a radar is consequently increased. However, for signals with PAPR very close to 0 dB, the transients of the signal become more rapid, possibly impractical [6]. The MIMO analysis shows that it is important to use signals with low PAPR and use PAs with high precision, in order to conserve the signals SINR.

With a good approximation of the PA, pre-distortion could possibly counteract the signal distortions caused by the PA. By implementing a small receiver directly after the PA, the amplified signal could be tuned using an adaptive filter in order to pre-distort the signal and achieve a better signal realization. As a lesser alternative to pre-distortion, by constructing a matched filter against the realized, transmitted signal, some of the SINR gain may be saved.



Issued by  
John Dahl and Sebastian Holmqvist  
Classification - Export Control  
NOT EXPORT CONTROLLED

Date                      Issue                      Document ID  
2013-06-11            A                              EX020/2013  
Classification - Company Confidentiality  
UNCLASSIFIED  
Classification - Defence Secrecy  
ÖPPEN/UNCLASSIFIED

---

## 7 Conclusions

The WAF is a robust method of matching signals that closely resembles the signal processing in a conventional radar. It shows that radar target detection is largely insensitive to the effects of the PA. Running the PA in compression produces similar results as lower input power levels.

Signal optimization towards lower PAPR allows for higher power efficiency in the PA. This increases the detection range. Also, signals with low PAPR are less susceptible to the harmful effects of the PA despite the large transients.

Optimal MIMO radar signals are susceptible to the effects of the class A-B PA and SINR is negatively affected.

Optimal MIMO radar signals could achieve better realizations by taking limitations of DACs and ADCs into account. ENOB, bandwidth, etc. are all important limitations in the hardware.

Pre-distortion would be possible in order to counteract the negative effects of the PA. This is especially true for signals optimized for a specific scenario. Further work is recommended.



Issued by  
John Dahl and Sebastian Holmqvist  
Classification - Export Control  
NOT EXPORT CONTROLLED

Date                      Issue                      Document ID  
2013-06-11            A                              EX020/2013  
Classification - Company Confidentiality  
UNCLASSIFIED  
Classification - Defence Secrecy  
ÖPPEN/UNCLASSIFIED

---

## References

- [1] Carlos Azeredo-Leme. Clock jitter effects on sampling: A tutorial. *Circuits and Systems Magazine, IEEE*, 11(3):26–37, 2011.
- [2] Neal Ciurro. Harmonics in industrial power systems. *EC & M*, 108(6):12–15, 2009.
- [3] Mathias Johansson. The hilbert transform. Master’s thesis, Växjö University, Gothenburg, 1999.
- [4] A. Malvino and D. Bates. *Electronic Principles with Simulation CD*. McGraw-Hill, Inc., 2006.
- [5] Steven W Smith. *Digital signal processing: a practical guide for engineers and scientists*. Newnes, 2003.
- [6] M. Ström. *Robust Transceiver Design and Waveform Synthesis for Wideband MIMO Radar*. PhD thesis, Chalmers University of Technology, Gothenburg, 2012.
- [7] Marie Ström, Mats Viberg, and Kent Falk. Robust transceiver design for wideband mimo radar utilizing a subarray antenna structure. *Signal Processing*, (0):–, 2013.
- [8] Robert H Walden. Analog-to-digital converter survey and analysis. *Selected Areas in Communications, IEEE Journal on*, 17(4):539–550, 1999.
- [9] M. Walker. The design of turbo field magnets for alternate-current generators with special reference to large units at high speeds. *Electrical Engineers, Journal of the Institution of*, 45(203):319–332, 1910.
- [10] L.G. Weiss. Wavelets and wideband correlation processing. *Signal Processing Magazine, IEEE*, 11(1):13–32, 1994.
- [11] Philip M Woodward. *Probability and information theory, with applications to radar*, volume 3. Pergamon Press London, 1953.
- [12] R.K. Young. *Wavelet theory and its applications*, volume 189. Springer, 1993.



Issued by  
John Dahl and Sebastian Holmqvist  
Classification - Export Control  
**NOT EXPORT CONTROLLED**

Date                      Issue                      Document ID  
2013-06-11      A                      EX020/2013  
Classification - Company Confidentiality  
**UNCLASSIFIED**  
Classification - Defence Secrecy  
**ÖPPEN/UNCLASSIFIED**

## A Equipment

The equipment used in the measuring rig is listed below in Table 7.

Inventory no.	Product name	Product type
A31698	Tektronix AWG520	Baseband generator
INV852558	Agilent E4433B	Signal generator
A41545	Tektronix TDS7404	Oscilloscope
—	Mini Circuits ZHL-3A	Bi-directional coupler
—	Werlatone C8356	Pre-amplifier
—	MRFE18010 Freescale	Active PA component
—	Hewlett Packard 437B	Power meter

Table 7: Measuring rig equipment.